Journal of Nuclear Materials 390–391 (2009) 528–531

Contents lists available at ScienceDirect

Journal of Nuclear Materials

journal homepage: www.elsevier.com/locate/jnucmat

Numerical modelling of steady-state fluxes at the ITER first wall

V. Kotov [a,*], A. Litnovsky [a], A.S. Kukushkin [b], D. Reiter [a], A. Kirschner [a]

[a] Institut für Energieforschung – Plasma Physik, Forschungszentrum Jülich GmbH, EURATOM-Association, Trilateral Euregio Cluster, D-52425 Jülich, Germany
[b] ITER Organization, Cadarache, France

ARTICLE INFO

PACS:
52.40.Hf
52.65.Pp
52.65.-y
28.52.Av

ABSTRACT

Plasma parameters in the vicinity of the ITER upper and equatorial ports have been modeled with B2-EIRENE code (SOLPS4.3). Erosion rates of Mo and W due to charge-exchange neutrals and deposition rates of C and Be have been estimated. The modelling results can be used for estimating the lifetime of the first mirrors of optical diagnostics and, to some extent, for evaluating the lifetime of metallic wall. Maximum calculated sputtering rate of Mo at the outer mid-plane is ≈0.005 nm/s, maximum calculated net deposition rate of Be is ≈0.01 nm/s. The modelling shows that gas puff can lead to significant local increase of erosion and decrease of deposition, ensuring the net erosion conditions for C and Be.

1. Introduction

This work was initially triggered by the need to estimate erosion and deposition rates at the elements of ITER diagnostic system located at the upper and equatorial ports [1]. Erosion can limit the lifetime of the first mirrors of optical diagnostics and deposition of impurities can lead to degradation of their optical properties. The mirrors will not experience a direct contact with plasma (they will be installed in protecting modules), therefore, their erosion and, to large extent, deposition will be due to neutral particles. Fluxes and energy spectra of the incident neutrals can be estimated rather reliably by Monte-Carlo codes.

In this work the B2-EIRENE code has been applied for this task. B2-EIRENE combines self-consistently a 2D fluid description of plasma with a Monte-Carlo kinetic model for neutrals. Since the design of the diagnostics is not yet completely defined, fluxes at the plasma-facing surfaces have been calculated as a first step (conservative estimate) and as a guideline for further work. The following questions have been addressed: (i) how large can be the sputtering by the fast atoms; (ii) how large can be the incident fluxes of impurities, especially Beryllium; (iii) what will be dominant: sputtering or deposition of impurities? Only steady-state plasma is considered (no transient events). To some extent the results of this work can be applied for estimating the first wall sputtering as well.

The paper is organised as follows. Section 2 contains a brief description of the model and modelling assumptions. Section 3 discusses the results and their implication for the mirrors. The conclusions are summarised in Section 4.

2. Modelling details

The modelling has been done with ITER version of B2-EIRENE code package (SOLPS4.3). It is a combination of the 2D multi-species fluid plasma transport code B2 ('Braams code') [2] and a 3D Monte-Carlo neutral transport code EIRENE [3]. Standard ITER model for neutral transport (from ITER design review modelling) is used [4–6], including neutral-neutral collisions and transport of line radiation. The model geometry and computational grid are shown in Fig. 1. Second separatrix is not taken into account: this simplification is commonly used in ITER modelling because it was found previously that including it does not increase significantly the wall loading at the top of the machine [7]. Due to technical limitations of the code the B2 grid on which plasma parameters are calculated is not extended up to the real wall location.

The model plasma consists of all charged species of D (representing both D and T), He, C and Be. Constant coefficients for cross-field transport are used: diffusivity 0.3 m^2/s for all species, thermal diffusivities 1 m^2/s for both electrons and ions. On the far-SOL boundary (outer edge boundary, flux surface closest to the wall) a decay length of 3 cm for temperatures and densities is prescribed. This simplified model for radial transport is applied in practically all studies made by ITER Team (see e.g. [4,8]). For continuity equation this combination of diffusivity and decay length corresponds to the fixed outflow velocity 10 m/s. Input power to the SOL is set to 100 MW. A full carbon divertor was assumed and a constant chemical sputtering yield of 1%.

Modelling cases and their salient parameters are listed in Table 1. Two types of the first wall have been considered: full carbon and full beryllium wall. For incident carbon particles full sticking is assumed on C surfaces but reflection on Be surfaces: to account for

* Corresponding author.
E-mail address: v.kotov@fz-juelich.de (V. Kotov).

0022-3115/$ - see front matter © 2009 Elsevier B.V. All rights reserved.
doi:10.1016/j.jnucmat.2009.01.301

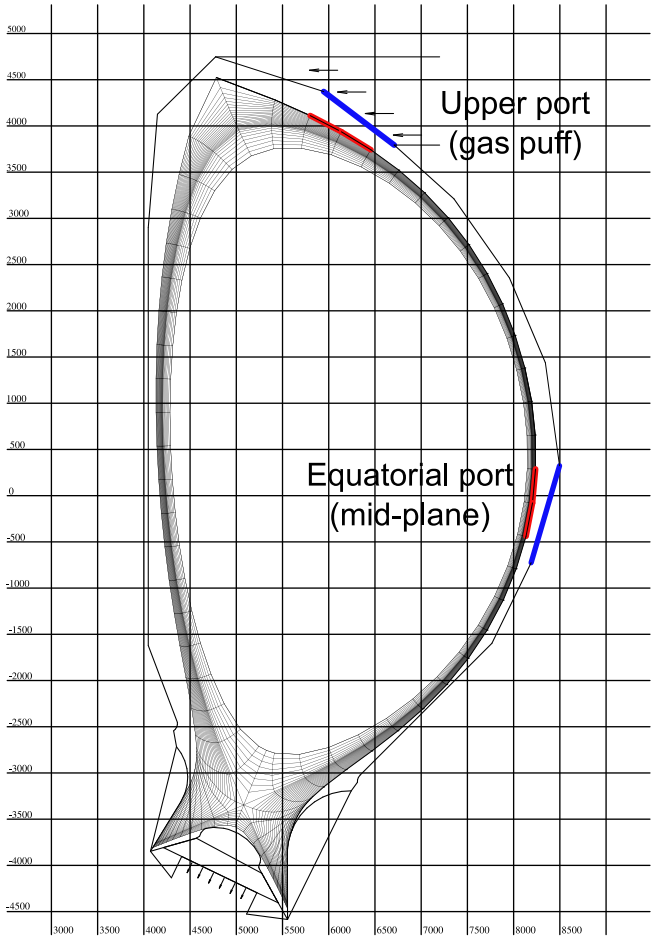

Fig. 1. B2 grid and positions of the diagnostic surfaces. Thick lines point out the locations of diagnostic surfaces on the grid edge (for ions) and first wall (for atoms).

Table 1
Modelling cases.

Notation	Γ_{inp}	P_{PFR}	q_{pk}	Z_{eff}	Wall
8e22,C	8e22	5.8	7.7	1.64	C
8e22,Be	8e22	5.9	7.8	1.59	Be
17e22,C	17e22	11.3	4.6	1.71	C
17e22,Be	17e22	10.7	5.6	1.70	Be
3e22,Be,CF	3e22	4.8	8.7	1.85	Be

Γ_{inp} (s^{-1}): *DT*-particle throughput (flux of nuclei); P_{PFR} (Pa): average neutral pressure in PFR; Z_{eff}: average effective charge at separatrix; q_{pk} (MW/m^2): peak target heat flux density; CF stands for core fueling.

re-erosion. For each wall type the regimes with low and high gas puffing rate (consequently, low and high divertor density) have been investigated. The gas puff is located at the upper port, pumping is prescribed from beneath the dome (modelled by specifying an absorption coefficient on the pumping surfaces). In this 2D modelling toroidal uniformity of the gas puff is assumed. One calculation has been made without gas puff but with increased particle flux from the core to simulate the core fueling by pellet injection.

Since the radial extension of the grid to the core region was relatively small (only 5 cm at the outer mid-plane) and an H-mode type transport barrier was not applied, the energy of neutral particles reflected from the core regions could be significantly underestimated. To roughly account for that in the diagnostic runs the neutrals which reached the core boundary were reflected back with a Maxwellian distribution with temperature 5 keV (expected temperature at the top of pedestal in ITER). Sensitivity of the result with respect to this assumption will be discussed in the next section.

The modelling was done in the following way. First, a coupled B2-EIRENE run is converged to get a self consistent (between plasma and neutral gas) solution. After that, a stand-alone diagnostic run of EIRENE is made. In this diagnostic run, the sputtering rates are calculated directly by the Monte-Carlo sampling: when a test particle hits the surface, its incident energy and angle are used to calculate the sputtering yield for different materials. Integral (sum) over all test particles yields the total sputtering rates. Eckstein–Roth–Bohdansky model for the rate of physical sputtering is used [9]. Angular dependence is taken into account by Yamamura fit, which yields a factor of 2 increase for oblique angles of incidence. No material mixing effects and enhanced sputtering of the deposited layers are taken into account. Sputtering due to atoms is calculated on the first wall surfaces, sputtering due to ions on the edge of B2 grid, see Fig. 1. No radial extrapolation is made for ion fluxes and plasma parameters. Ion depositing fluxes are calculated on the grid edge as well.

3. Results and discussion

The plasma parameters at the divertor targets are almost the same in the cases with carbon and beryllium wall (for the same divertor density), see e.g. q_{pk} in Table 1. Total radiated power (50–65 MW) does not change when switching from C to Be wall, since it mainly comes from carbon sputtered in the divertor. In the case with core fueling the divertor is hotter, because the total throughput and divertor neutral pressure are smaller than in the 'gas puffing' cases. In order to achieve realistic divertor heat loads with core fueling the pumping albedo was reduced from 0.7% to 0.3% (this corresponds to decreased pumping speed), therefore, the impurity removal worsened as well, see Z_{eff} in Table 1.

Radial plasma profiles at the equatorial (outer mid-plane) and upper ports (in front of the gas puff) are shown in Fig. 2. Despite the assumption of fully diffusive transport, the density profile in the far-SOL is relatively flat and the density reaches $\sim 10^{19}\ m^{-3}$, Fig. 2(d), sustained by recycling. In the upper port the particle flux density due to (toroidally uniform) puffing can exceed that due to recycling by more than an order of magnitude. Therefore, the local effect of gas puff is significant. The density profile has a well pronounced maximum, Fig. 2(a). The temperature at the grid edge can drop down to 2 eV, Fig. 2(b,c). With Be wall the density in the far-SOL is higher because of the increased electron source due to sputtered Be and re-eroded (in the model – reflected) C. Despite much lower particle throughput, the separatrix density in the case with core fueling is the same as with gas puff, but the radial density gradient is somewhat larger.

Calculated incident fluxes, sputtering and deposition rates are shown in Table 2. In the text below, if the opposite is not stated, only sputtering due to incident atoms is considered. Calculated incident ion flux density Γ_{DT^+} at the mid-plane is $(4–8)\times 10^{19}\ m^{-2}/s$ with gas puff and $2.4\times 10^{19}\ m^{-2}/s$ with core fueling. Incident flux of atoms takes approximately 50% of the ion flux. Maximum sputtering rate is 5×10^{-3} nm/s for Mo and 3×10^{-3} nm/s for W. This value could be underestimated because of the assumption on radial transport used in the present work. Experimental data indicate that the transport in the far-SOL is likely to be dominated by intermittent events (blobs), and the time-averaged velocity of radial convection (deduced from the measured radial profiles) can reach 30–100 m/s [10,11], which is far above the outflow velocity 10 m/s assumed here. As a first approximation one can make use of the fact that the ratio of sputtering rate to Γ_{DT^+} is rather insensitive (varies only within a factor

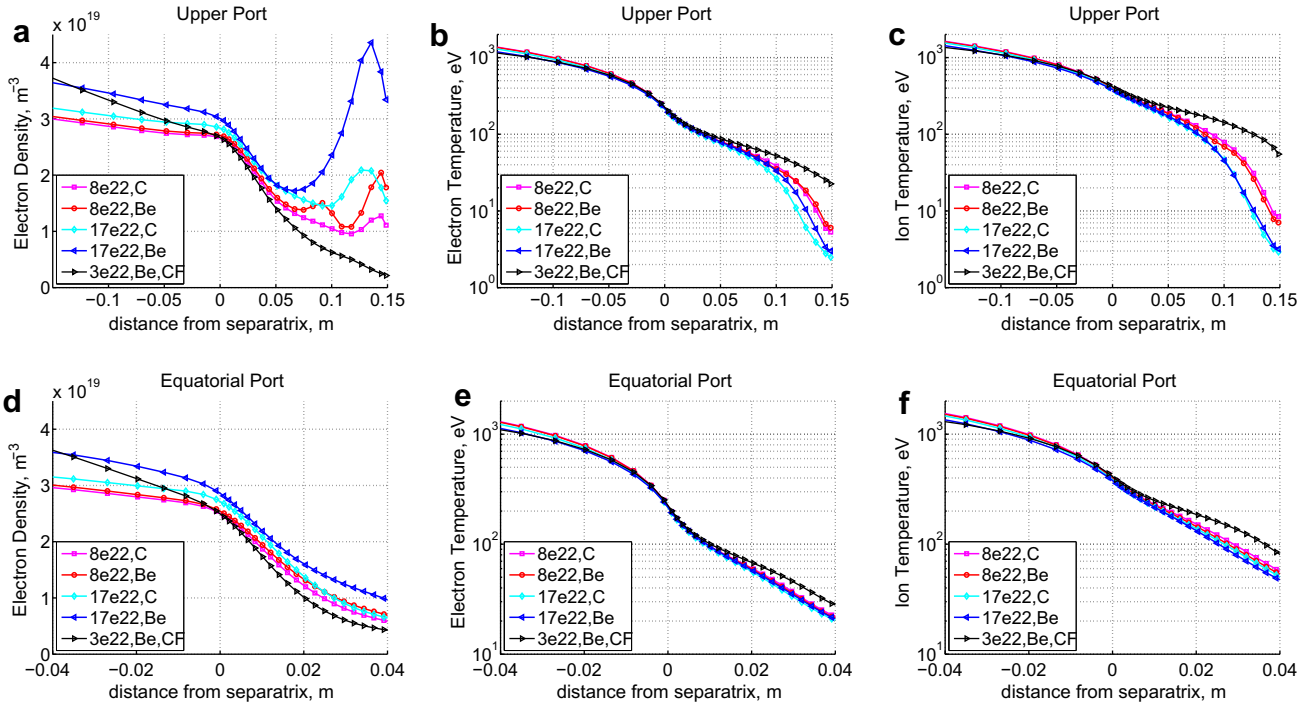

Fig. 2. Radial plasma profiles in front of the upper and equatorial (outer mid-plane) ports: electron density, electron and ion temperature (the model did not contain edge transport barrier).

Table 2
Calculated incident fluxes (Γ, m^{-2}/s), sputtering[a] (S) and deposition[b] (D) rates (nm/s).

Case	Γ_{DT^+}	Γ_{DT}	S_C	S_{Be}	S_{Mo}	S_W	D_C	D_{Be}
Equatorial port (mid-plane)								
8e22, C	4.1e19	2.4e19	4.9e−3	4.5e−3	4.5e−3	2.5e−3	2.6e−2	0e0
8e22, Be	5.1e19	2.8e19	5.5e−3	4.9e−3	4.6e−3	2.5e−3	2.6e−2	1.1e−2
17e22, C	4.6e19	2.8e19	5.3e−3	4.9e−3	4.4e−3	2.4e−3	3.0e−2	0e0
17e22, Be	7.8e19	4.1e19	7.6e−3	6.9e−3	5.4e−3	2.8e−3	2.2e−2	1.4e−2
3e22, Be, CF	2.4e19	1.1e19	2.3e−3	2.0e−3	2.3e−3	1.2e−3	3.1e−2	5.3e−3
Upper port (gas puff)								
8e22,C	1.1e20	6.7e20	8.2e−2	7.5e−2	1.5e−2	5.0e−3	1.2e−2	0e0
8e22,Be	1.8e20	7.7e20	8.5e−2	4.3e−2	1.1e−2	3.8e−3	7.8e−5	7.6e−3
17e22,C	1.7e20	1.6e21	1.7e−1	1.6e−1	2.1e−2	7.0e−3	2.4e−2	0e0
17e22,Be	3.3e20	1.7e21	1.6e−1	3.4e−2	6.3e−3	2.3e−3	2.7e−4	6.6e−3
3e22,Be,CF	1.1e19	5.6e18	1.0e−3	9.1e−4	5.5e−4	1.8e−4	1.6e−2	3.0e−3

[a] Only due to incident atoms.
[b] Sum over all charged states and neutrals.

of 2 for different cases). Therefore, to account for the possibly underestimated Γ_{DT^+} a safety factor 10 (factor of ignorance) have to be introduced, and the calculated sputtering rates can be scaled with this factor.

At the upper port the incident fluxes can be higher due to local influence of gas puff. For the largest gas puffing rate the calculated Γ_{DT^+} reaches 3.3×10^{20} m^{-2}/s for Be wall and 1.7×10^{20} m^{-2}/s for C wall. Maximum incident neutral flux density is 1.7×10^{21} m^{-2}/s, but the energies are lower than at the mid-plane, see Fig. 3. As a result, the sputtering rates are only several times higher: the maximum is $\approx 2 \times 10^{-2}$ nm/s for Mo and $\approx 7 \times 10^{-3}$ nm/s for W. The effect of radial transport at this location could be less important than at the mid-plane. However, in reality the gas puff will not be completely toroidally uniform and the incident fluxes could be affected by the position of the diagnostic port with respect to the gas puff. Without gas puff conditions at the upper port are close to those at the mid-plane.

To check sensitivity of the results to the boundary condition at the core boundary, the diagnostic runs were repeated assuming

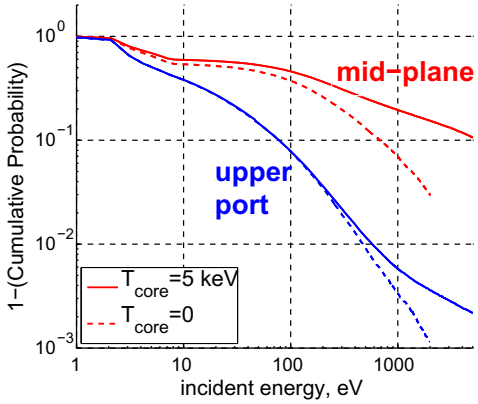

Fig. 3. Energy spectra of the incident atoms (integral over all angles of incidence). Modelling case '8e22, C', two locations. The plotted function $F(E)$ shows the fraction of atoms which have energy larger than E. '$T_{core} = 0$' stands for the case with absorbing core boundary.

full absorption of neutrals at this surface. The sputtering rates of Be and C did not change (as expected). The maximum decrease of the sputtering rate at the upper port is a factor of 2.1 for Mo and a factor of 2.8 for W. At the equatorial port: a factor of 3 for Mo and a factor of 5.4 for W. The effect is much smaller for the cases with Be wall than for the C wall because of higher density and more efficient screening of neutrals: only a factor of 2.1 difference for W at the mid-plane. An example of the energy spectra of incident atoms at the upper and equatorial ports is shown in Fig. 3. At the mid-plane the amount of particles with energies >1 keV can change by a factor 2–3 when different boundary conditions are applied (sputtering rates of Mo and W have maximums about 1 keV and then slowly decrease for higher energies). At the end, the sputtering rate of W, maximal over all cases, is only a factor of 2 smaller when absorbing of neutrals at the core boundary is assumed.

The results of the present paper can be compared to work [8]. In this latter the issue of the ITER first wall lifetime was addressed. B2-EIRENE with old model for neutral transport was used. It had, in particular, more primitive description of the hydrogen molecular chemistry which did not take into account electronic and vibrational excitations and elastic collisions of molecules with ions. This old model also did not include neutral-neutral collisions and radiation opacity, but this can have only indirect influence on the first wall sputtering via modification of the plasma parameters in divertor and radial profiles. The geometry and SOL power were the same as in the current work, but the grid was extended further to the core. Full carbon wall was assumed, no Be in plasma. Besides that, a different way of calculating the incident spectrum of neutral particles was used: integration along diagnostic chords [12], replaced in the present work by a direct sampling. Chords integration allows better numerical accuracy, but physically less accurate (uses extra model assumptions). Sputtering rates on the outer mid-plane obtained in [8] were: $\approx 2 \times 10^{-2}$ nm/s for Mo and $\approx 8 \times 10^{-3}$ nm/s for W (the poloidal variation is weak). In the present paper, the calculated total sputtering rates (due to both atoms and ions) at the outer mid-plane are 10^{-2} nm/s for Mo and $(4–5) \times 10^{-3}$ nm/s for W. Therefore, the agreement between two works is withing a factor of 2.

As a side result of the present work, the total effective sputtering yield of metallic first wall can be estimated: the ratio of the total sputtered flux and Γ_{DT^+}. At the outer mid-plane it is equal to $(0.8–3.3) \times 10^{-2}$ for Mo and $(0.5–1.3) \times 10^{-2}$ for W. Charge-exchange neutrals contribute roughly half to the total sputtering, the rest is (in the model) due to impurities accelerating in the sheath potential. Near the gas puff almost entire calculated sputtering is due to incident neutrals.

The total deposition rates of C and Be have been estimated assuming full sticking. Elastic collisions of C and Be atoms with ions are not included in the model, therefore, the total calculated flux (sum over all charged states) is taken as an upper estimate. The maximum calculated deposition rate of C is 3×10^{-2} nm/s at both locations. For Be this rate is $\approx 8 \times 10^{-3}$ nm/s near the gas puff, and $\approx 1.4 \times 10^{-2}$ nm/s at the mid-plane. The deposition rate is reduced near the gas puff due to thermal force which pushes impurities away from the low temperature region.

It is important to find out, if net erosion or deposition is to be expected at the mirror. It has been found, that with gas puff the sputtering rates of Be and C due to charge-exchange neutrals exceed the deposition rates by at least a factor ≈ 4. Therefore, the deposited layers can probably be re-eroded. At the equatorial port the sputtering due to neutrals is always more than a factor of 2 smaller than deposition. Therefore, net-erosion of Be and C is not guaranteed.

Uncertainties in Γ_{DT^+} and C chemical sputtering yield should not significantly affect this conclusion, because both deposited and sputtered fluxes change simultaneously. In the paper [13] the results of UEDGE modelling (2D plasma fluid code with fluid model for neutrals) were used to calculate incident fluxes at the ITER outer mid-plane. In this modelling [14,15] a radial convective velocity 70 m/s in the far-SOL was specified on the low field side. The resulting incident flux Γ_{DT^+} is 4×10^{20} m^{-2}/s, thus, by an order of magnitude higher than in the present paper. However, the calculated total flux of Be ($\Gamma_{Be^{0.4+}} = 1.4 \times 10^{19}$ m^{-2}/s) was an order of magnitude higher as well. The concentration $c_{Be} = \Gamma_{Be^{0.4+}}/\Gamma_{DT^+} = 0.035$ is in a good agreement with the results of the present paper (c_{Be} = 0.022–0.028), giving some confidence in the normalized impurity fluxes.

4. Conclusions

In this work sputtering and deposition rates at the ITER upper and equatorial ports have been estimated using B2-EIRENE modelling. Only steady-state conditions have been considered (no ELMs and disruptions). The focus has been made on the implications for the first mirrors of optical diagnostics. A conservative upper estimate has been taken by considering fluxes at the plasma-facing surface. The maximum calculated erosion rate of Molybdenum at the mid-plane is 2 μm/year (1 year = 1000 shots × 400 s), for Tungsten this value is only ≈2 times smaller. Experimental data from modern tokamaks indicate, that the incident plasma flux resulting from the transport model used in this work could be underestimated and the calculated sputtering rates should be multiplied by a safety factor (engineering margin) 10. In the upper port the calculated erosion rate can become several times larger due to local influence of the gas puff. The calculated maximum deposition rate of Beryllium is 0.014 nm/s at the mid-plane and a factor of 2 smaller near the gas puff. To get 'the most pessimistic estimate' it should be multiplied by the factor of 10 as well. Deposition rates of Carbon have the same order of magnitude. It has been shown that at the upper port with gas puff the erosion due to charge-exchange neutrals could be sufficient to achieve net erosion of Beryllium and Carbon at the mirror.

The calculations made in this work did not take into account toroidal non-uniformity of the gas puff and real geometry of the diagnostic duct. 3D modelling is required to get more reliable estimates of the erosion and deposition at the mirror itself and to optimise the design. Such a modelling can be performed with the kinetic Monte-Carlo neutral transport code EIRENE.

References

[1] A. Litnovsky et al., Nucl. Fus. 47 (2007) 833.
[2] B.J. Braams, Ph D Thesis, Rijksuniversitet Utrecht, 1986.
[3] D. Reiter, M. Baelmans, P. Börner, Fus. Sci. Technol. 47 (2005) 172. <http://www.eirene.de>.
[4] A.S. Kukushkin, H.D. Pacher, et al., Nucl. Fus. 45 (2005) 608.
[5] V. Kotov, D. Reiter, et al., Contribution Plasma Phys. 46 (2006) 635.
[6] V. Kotov, D. Reiter, A.S. Kukushkin, Report Jül-4257, 2007. <http://www.eirene.de/kotov_solps42_report.pdf>.
[7] A.S. Kukushkin, H.D. Pacher et al., in: Proceedings of the 26th EPS Conference on Contribution Fusion and Plasma Physics, Maastricht, vol. 23J, 14–18 June 1999, ECA, 1545.
[8] R. Behrisch, G. Federichi, et al., J. Nucl. Mater. 313–316 (2003) 388.
[9] W. Eckstein, J. Bohdansky, J. Roth, in: Nuclear Fusion Special Supplement, Atomic and Plasma-Material Interaction Data for Fusion, vol. 1, International Atomic Energy Agency, Vienna, 1991, 1991, p. 5.
[10] A. Kallenbach, R. Neu, et al., Plasma Phys. Contr. Fusion 47 (2005) B207.
[11] B. Lipschultz, X. Bonnin, et al., Nucl. Fusion 47 (2007) 1189.
[12] H. Verbeek, J. Stober, D.P. Coster, et al., Nucl. Fusion 38 (1998) 1789.
[13] J.N. Brooks, J.P. Allain, Nucl. Fusion 48 (2008) 045003.
[14] T.D. Rognlien et al., J. Nuclear. Mater. 363–365 (2007) 658.
[15] J.N. Brooks, J.P. Allain, T.D. Rognlien, Phys. Plasm. 13 (2006) 122502.